Ch.2 Optical Properties of Biological Tissues

2.1 Optical Properties of Biological Tissues

2.1.1 Skin

2.1.2 Eye

2.1.3 Muscle

2.1.4 Fat

2.1.5 Brain

2.1.6 Tumor tissues

2.2 Laser Safety

2.1 Optical Properties of biological tissues

When the EM wave of optical ray encounters the biological tissue, there will be multiple effects of reflectance, absorption, and scattering due to inhomogeneity of the sample. To characterize the properties of biological tissue, there are four parameters of optical properties can be derived from directed or indrected measurement of biological tissues, e.g. refractive index n, absorption coefficient u_a, scattering coefficient u_s, and anisotropy factor, g. Even though, each tissue has its own characteristic optical absorption spectra, one can approximate the optical properties of tissues with that of water, due to the facts of water is the major composition of human body, > 70%. Both water and saline solution transmit well in the visible range and the absorption is high in the UV (?<300 nm) and the IR (?>2um). Tissue shows similar strong absorption in the UV and the IR.

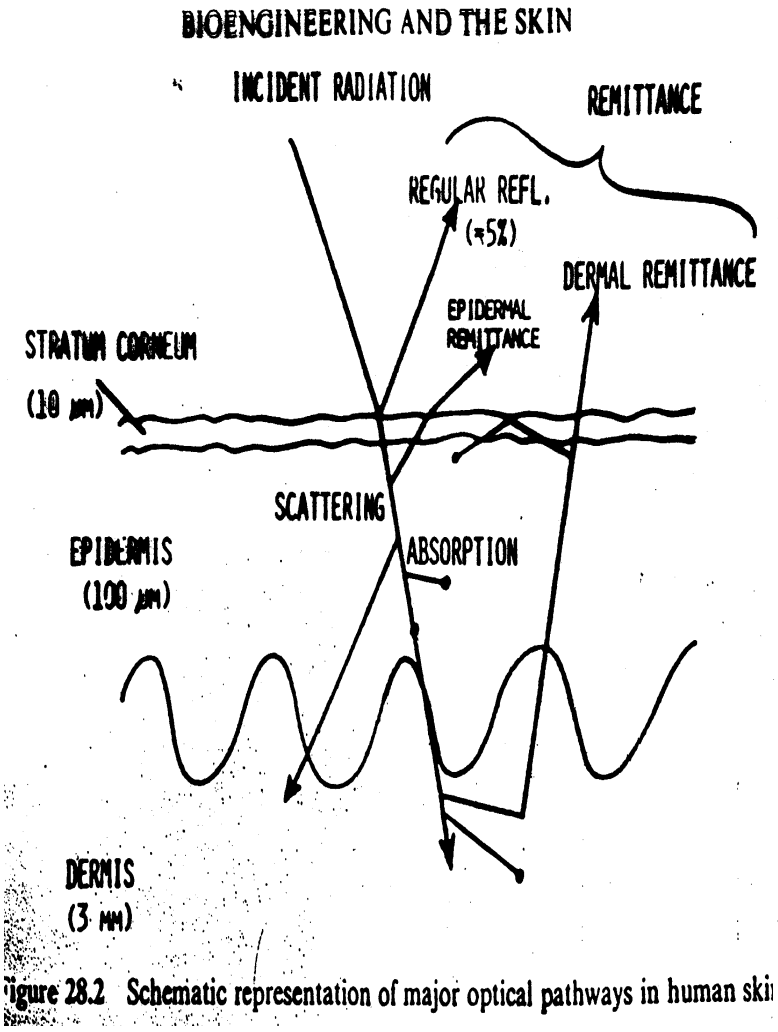

Figure 28.2 Schematic representation of major optical pathways in human ski

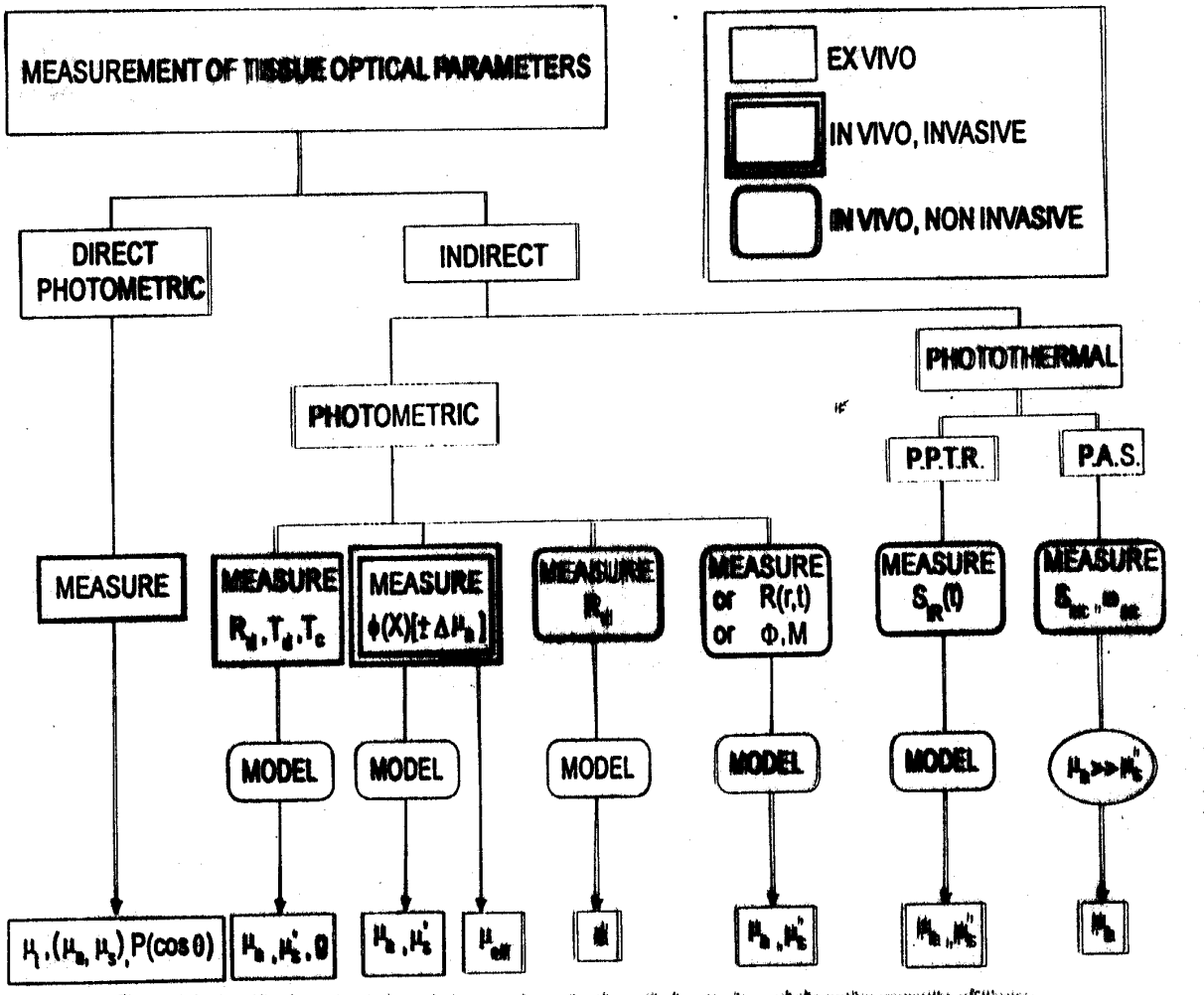

Figure 8.1. Classification scheme for techniques to determine the optical scattering and absorption properties of tissues.

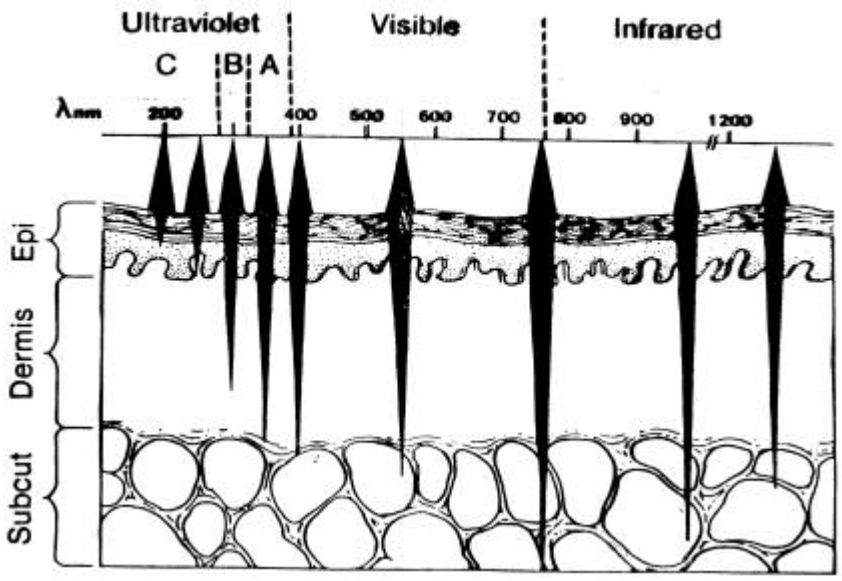

Approximate depth for penetration of optical radiation in fair Caucasian skin to a value of 1/e (37%) of the incident energy density

Wavelength (nm)	Depth (μm)
250	2
280	1.5
300	6
350	60
400	90
450	150
500	230
600	550
700	750
800	1200
1000	1600
1200	2200

However in blood, there are strong absorption in the visible range due to chromophores (**色素基**) such as hemoglobin (**血紅素**) and bilirubin（**膽紅素**）. Therefore for a tissue that contains blood, the absorption is dominated by the absorption in the blood. There are also other chromophores that absorb light in the specific spectral range, such as melanin（**黑色素**）and proteins as shown in the following figure.

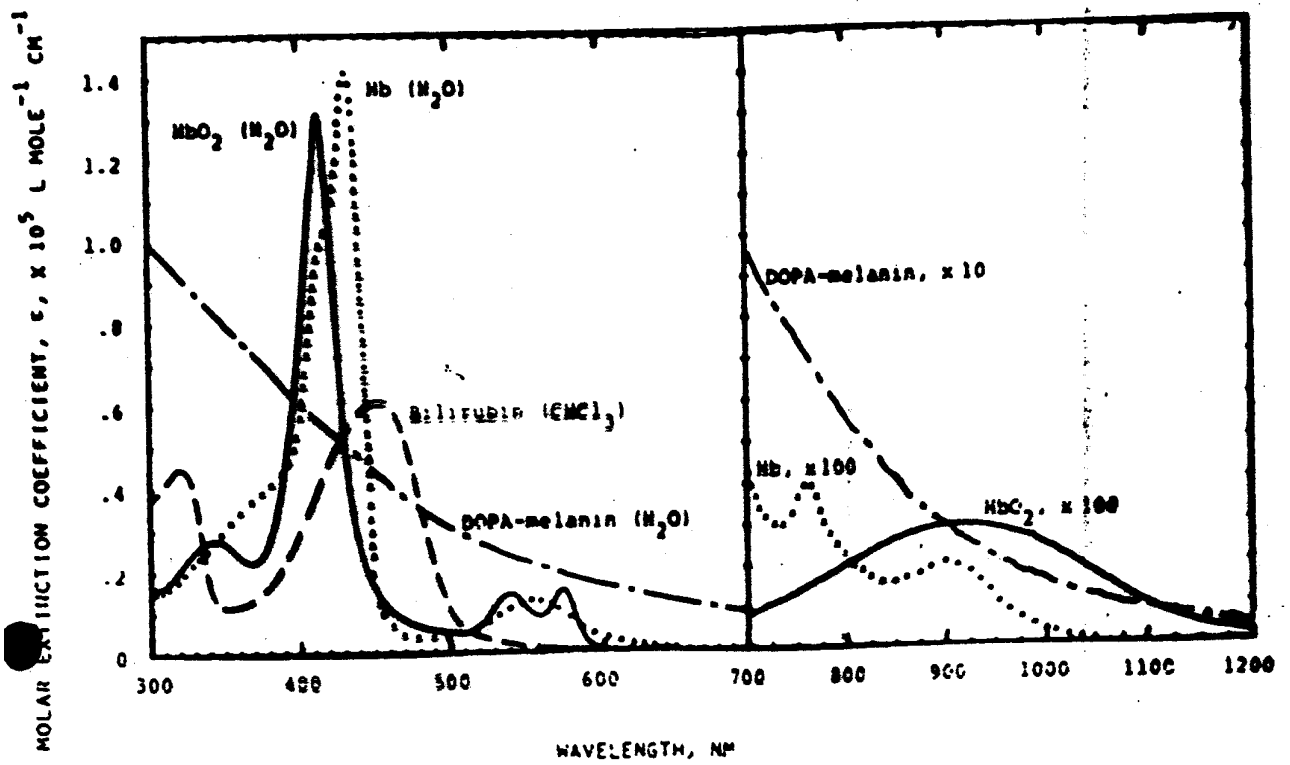

FIG 8. Absorption spectra of major visible-absorbing pigments of human skin, HbO_2 (——), Hb (. . . . .), bilirubin (- - - - -), and DOPA-melanin (—·—). Parentheses indicate solvent. The spectrum shown for DOPA-melanin is the absorbance on a scale of 0 to 1.5 of 1.5 mg% aqueous solution. Not shown is β-carotene, which has a broad absorption band qualitatively similar to that for bilirubin in the 400–500 nm region, with maxima at 466 and 497 nm in $CHCl_3$. Note scale changes in the near infrared.

Due to the difference in isotropic and intracellular contents, different types of tissue do show markedly different optical and thermal properties. It thus requires in depth investigation for the clinical applications of optical methods. Some of these properties may depend on the water content of the tissue. For example, during laser vaporization of tissue, the water content change, causing the optical properties to vary. The fundamental optical properties of interest are the absorption coefficient, u_a, scattering coefficient, u_s, total attenuation coefficient, $u_t = u_a + u_s$, scattering phase function, p(cos?), or scattering anisotropy, *g*, reduced scattering coefficient, $u_s' = u_s(1-g)$, the tissue refractive index, *n*, and the effective attenuation coefficient, u_{eff}. For most of the soft tissue, reflective index is around 1.37 – 1.45. ($C' = c_0/n$, for n=1.4, c' = 0.21 mm/ps). However, there has been an extensive review on various biological tissues and various wavelengths [1].

Ref: Cheong et.al. "A review of the optical properties of biological tissues", 1990, IEEE J. Quantum Electronics 26: 2166-2184

2.1.1 Skin:

Skin consists of three main layers: (1) the epidermis（表皮 50-150 um）, separated from the underlying dermis by a basement membrane（基底層）, (2) the dermis（真皮） (1000-4000 um), with collagen （膠原蛋白）and elastic fibers produced by fibroblasts（纖維母細胞）, blood and lymph vessels, hair follicles（毛囊）, sweat and sebaceous glands（皮脂腺）, smooth muscles, and nerves, (3) the subdermal tissue, consisting of a fat layer.

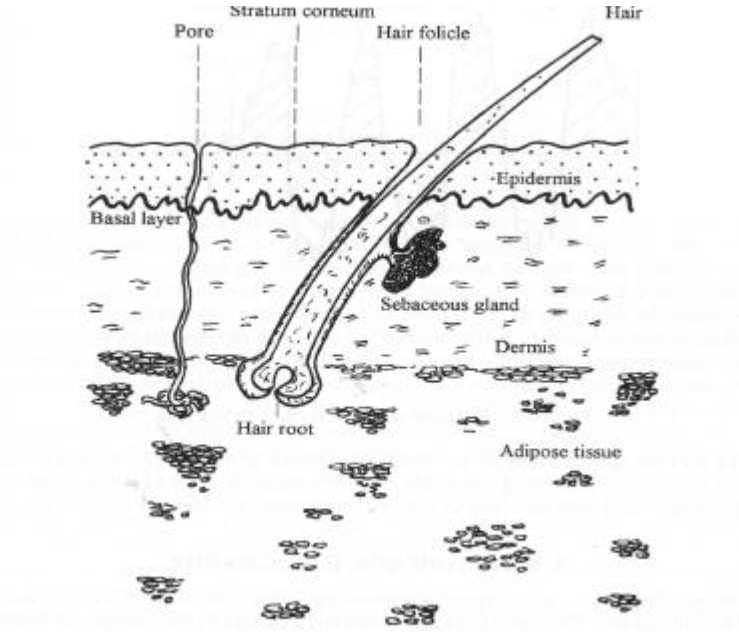

Figure 1 The structure of skin.

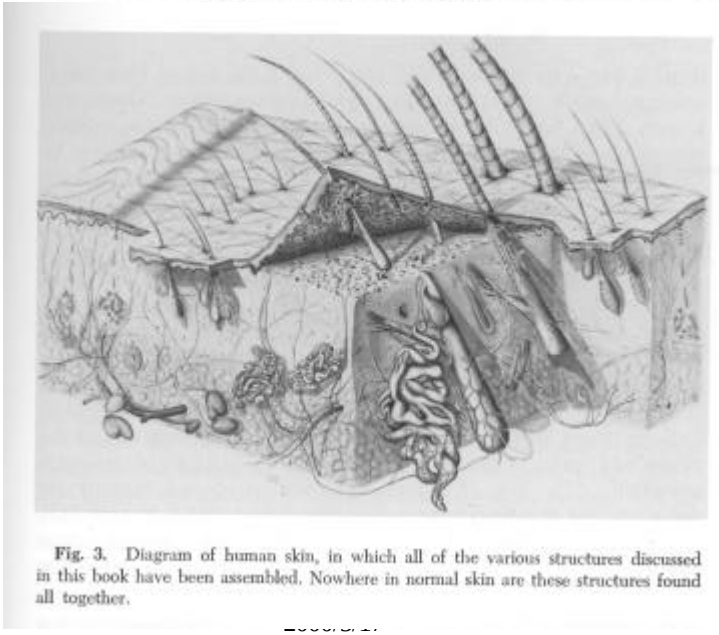

Fig. 3. Diagram of human skin, in which all of the various structures discussed in this book have been assembled. Nowhere in normal skin are these structures found all together.

2.1.1.1 **The epidermis of the skin consists of four layers**: (1) The basal layer (stratum germinativum（生長層）, where division occurs (5-10 um thick), (2) the stratum spinosum（棘突層）, consisting of keratinocytes （角質細胞） with intercellular bridges (50-150 um), (3) the granular layer (stratum granulosum（粒層）), where keratohyalin（角質層透明質）granules are formed (3um), and (4) the stratum corneum（角質層）, where anucleated （無核）cells form a protective layer (8-15 um). The bottom three layers of epidermis can also be called Malpighian layer (living). Melanocytes （黑色素細胞）are dendritic cells located in the basal

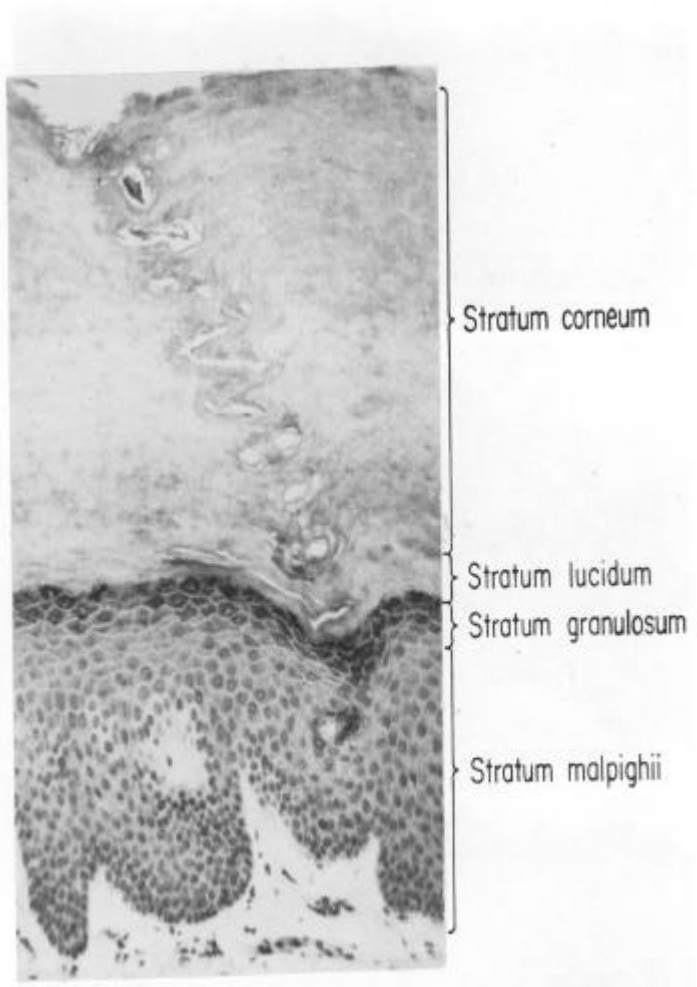

Fig. 2. Epidermis from the palm showing all of its layers. The clefts in the horny layer are fragments of the spiralling duct of an eccrine sweat gland.

layer. Their processes extend up into the malpighian layer. Melanocytes and melanin-loaded malpighian cells (keratinocytes) compose the epidermal melanin unit. The thickness and arrangement of the epidermis can have difference from different locations of the body.

2.1.1.2 **Optical Properties**: The regular reflectance of an incident beam normal to skin is 4-7% over the spectrum from 250 to 3000 nm. This gives rise to the skin color perception. At lower angle incidence, higher reflectance is expected by the Fresnel equations. The fraction of normally incident radiation entering the skin is 93-96%. Within any layer of the skin this radiation

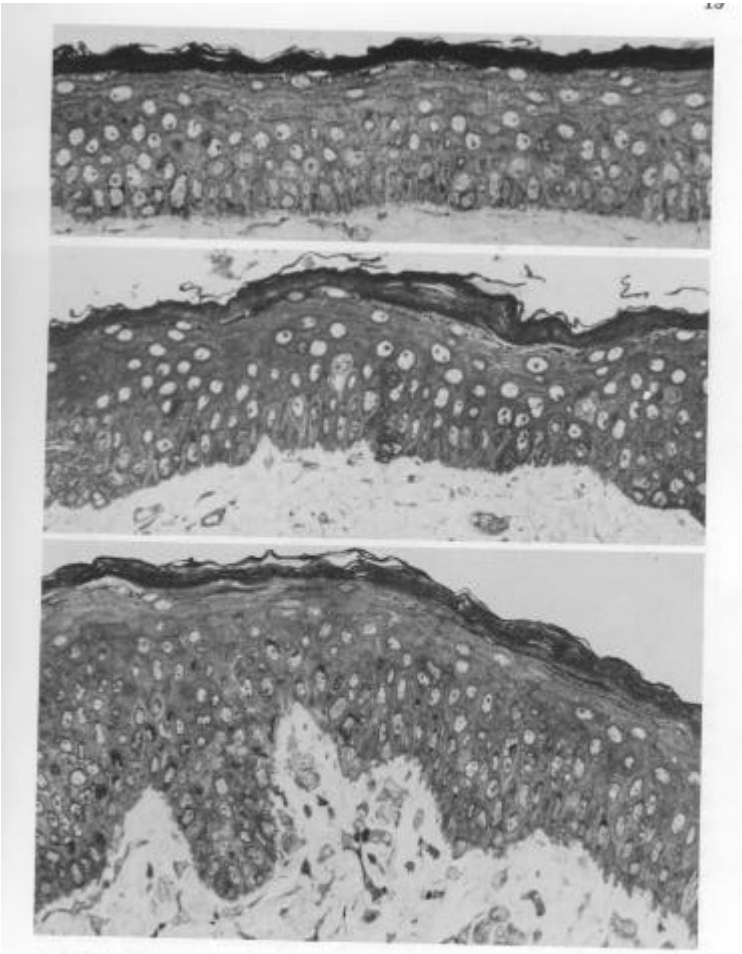

Fig. 1. The epidermis from the cheek (above), behind the ear (middle), and labia majora (below) showing the compact horny layer above and the Malpighian layer below. The horny layer is intact and compact. The differences in dermo-epidermal junction are characteristic of these areas. (Courtesy of Dr. M. Bell.)

may be absorbed or scattered. Melanin, which absorbs uniformly over the visible wavelengths, acts as a neutral density filter to diminish dermal remittance. Blood within the dermis scatters the longer wavelengths and absorbs the blue-green wavelengths, resulting in a reddish hue. UV radiation shorter than 320 nm is absorbed by proteins, DNA, and other constituents of epidermal cells. In Caucasian skin, at least 20-30% of the incident radiation in the sunburn range (290-320 nm) reaches the malpighian cells, and probably 10% penetrates to the upper dermis. The stratum corneum of black skin absorbs a greater amount of UVB radiation due to melanin.

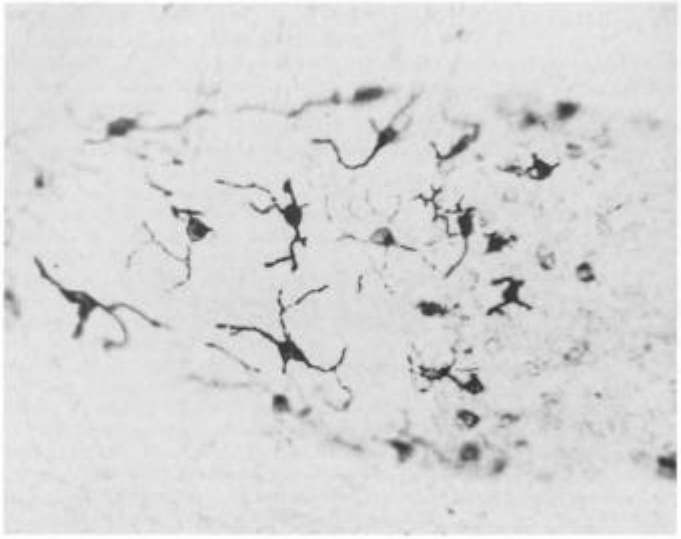

Fig. 1. Melanocyte in a lactiferous duct of a young woman.

2.1.1.3 **Photodamage**: The UV-visible transmission of the Caucasian stratum corneum and epidermis is affected by tryptophan（色氨酸）, tyrosine（酪氨酸）, and other aromatic （芳

香族）chrophores that absorb near 280 nm. Nucleic acids (absorption maximum near 260 nm) and urocanic （尿色素）acid (max. at 277 nm at pH 7.4) also contribute to the 280 nm absorption band. While the degree of absorbance of the stratum corneum and epidermis below 250 nm is largely due to peptide bonds. It is thus a critical protection mechanism by melanogenesis and epidermal hyperplasia. Melanin absorption steadily increases from 250 to 1200 nm. Beyond 1100 nm, both transmittance and remittance are unaffected by melanin. The prevalence of sunburn, abnormal photosensitivity, skin cancer, and cutaneous “aging” decreases with increasing melanin concentration. The transmission of dermis is affected by the existence of collagen, which has the same order of the wavelength of light and causes scattering effect. Longer wavelengths exhibit both greater and more forward-directed (less diffuse) transmission. Two optical “windows” exist in skin: between 600 –1200 nm (high dermal scattering and absorption for <600 nm) and at 1600-1850 nm, between the two water absorption bands. At the windows, the volume and depth of tissue affected by photoxicity will be large.

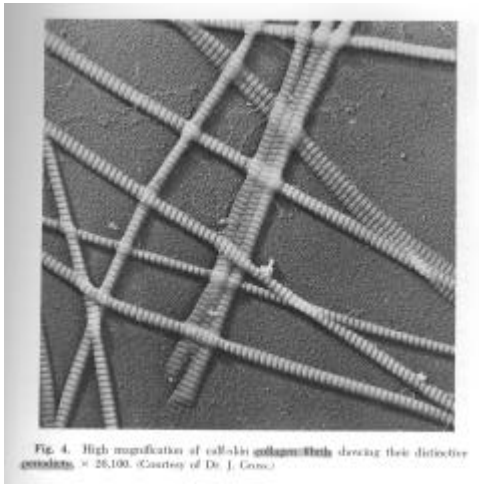

Fig. 4. High magnification of collagen fibrils showing their distinctive periodicity. × 26,100. (Courtesy of Dr. J. Cross.)

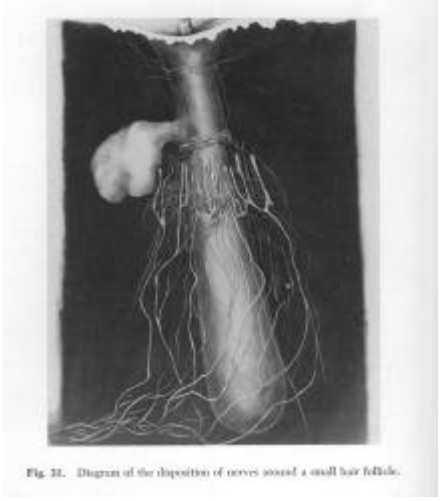

Fig. 31. Diagram of the disposition of nerves around a small hair follicle.

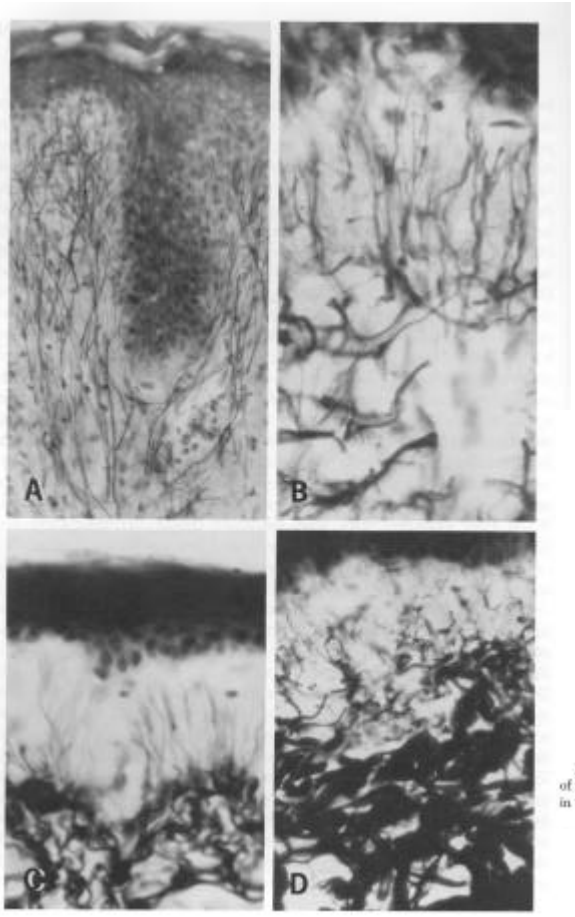

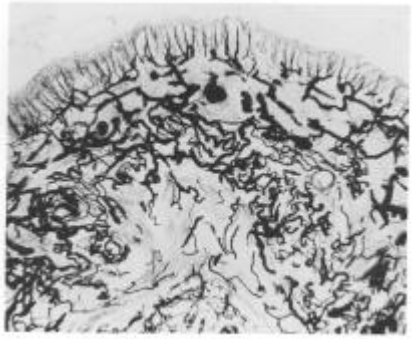

Fig. 3. 1 100-μm section from a toe injected with India ink. Compare this specimen with the diagram in Fig. 2. (Courtesy of Dr. R. K. Winkelmann.)

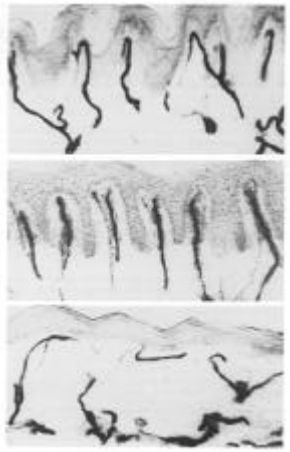

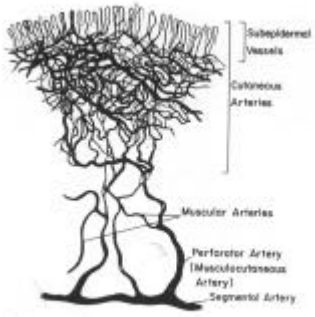

Fig. 2. Diagram showing the patternless cutaneous vascular system, the branching of the segmental artery into the perforator (musculocutaneous) artery, and the latter, in turn, branching into muscular and cutaneous arteries.

2.1.2 Eye

"The eye has every possible defect that can be found in an optical instrument and even some which are peculiar to itself; but they are so counteracted, that the inexactness of the image which results from their presence very little exceeds, under ordinary conditions of illumination, the limits which are set to the delicacy of sensation by the dimensions of the retinal cones' (Helmholtz, 1962).

2.1.2.1 The standard eye: The globe of the adult eye can be approximated as a sphere with an average radius of ~12 mm. It is completed anteriorly by the transparent cornea, which forms a roughly spherical cap with a radius of ~8 mm.

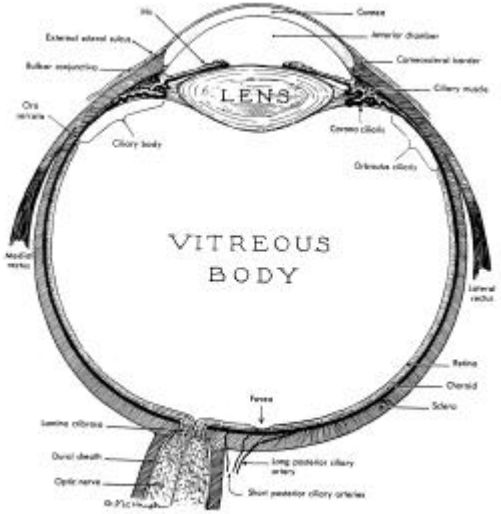

2.1.2.2 Cornea (n=1.376): The vertical and horizontal

diameters of the adult cornea are about 12 and 11 mm respectively. It is covered by a thin tear film, some 6-10 um thick. The cornea is made up of several distinct layers – the epithelium, Bowman's membrane, the stroma, Descemet's membrane and the endothelium. The stroma makes by the greatest contribution (~90%) to the overall thickness of about 0.5 mm at the center of the cornea and 0.7 mm at the periphery. The constituent collagen fibers, each 25-33 nm in diameter, are arranged in the stroma. Not only their structure and arrangement lead to birefringence(**雙折射**) but also their quasiuniformsize and regularity are of vital importance to corneal

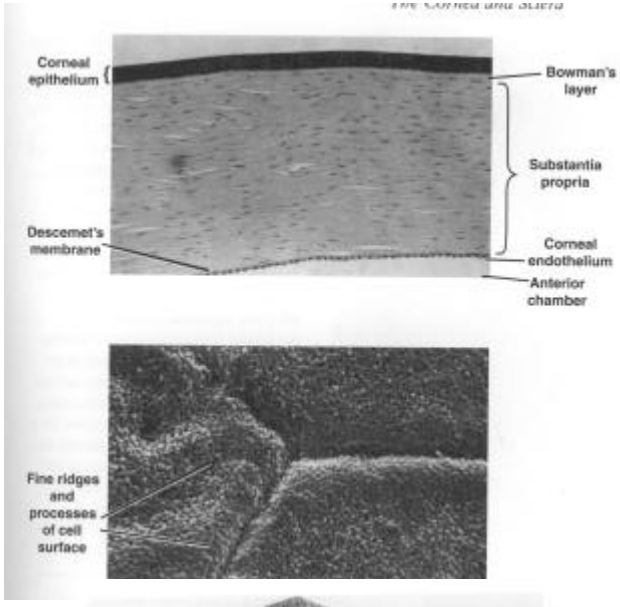

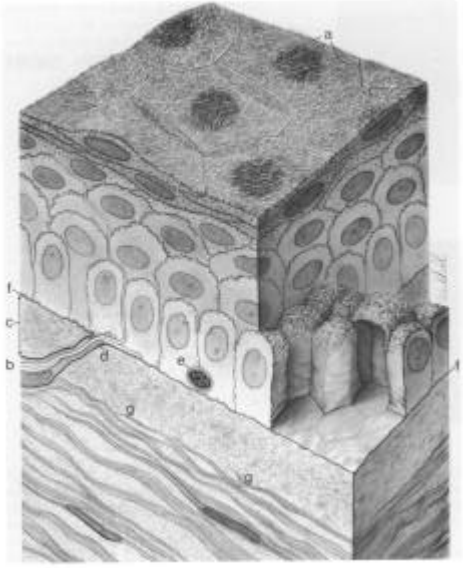

transparency. The fibers form regular lattices. Thus, although scattering occurs from each fiber due to differences in refractive index between the fibers and the interstitial material the resultant scattered light from the overall lattice interferes destructively in all directions except that of the incident radiation, leading to good corneal transparency unless the regularity of the stromal lattice is distributed by oedema or trauma. (as in the cataract case **白內障**)

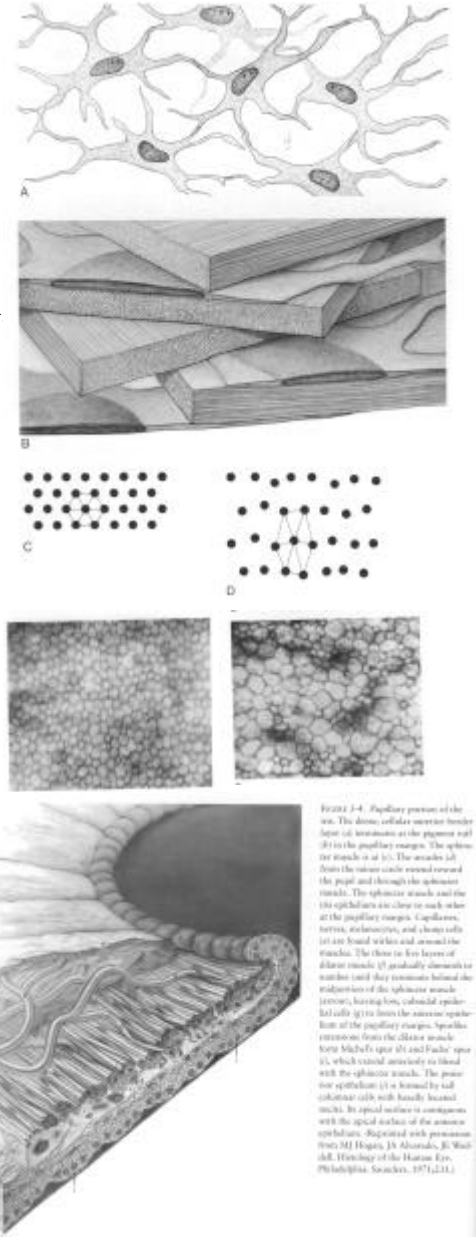

2.1.2.3 Aqueous humour (n=1.337): It is a clear transparent liquid, constitute of extracellular optical medium, scattering very little light unless cellular debris accumulates as the result of pathology or the after effects of surgery.

2.1.2.4 Pupil: It plays the important role of aperture stop to the

optical system of the eye with adjusting the size from 2 – 7 mm approximately. It controls the dynamical range of the eye response to ambient light changes.

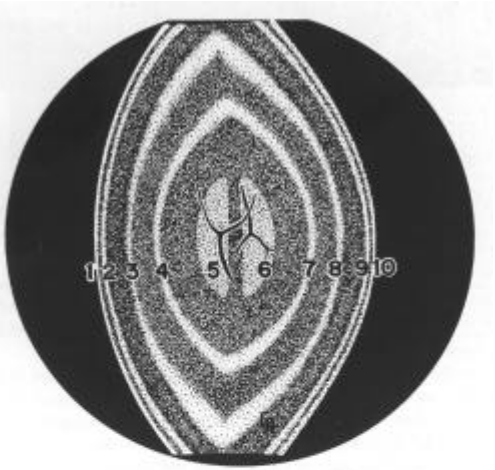

FIGURE 5-7. Optical section of normal adult lens. (*1*) Anterior capsule; (*2*) anterior line of disjunction; (*3*) anterior surface of adult nucleus; (*4*) anterior surface of fetal nucleus; (*5*) inner layer of anterior half of fetal nucleus, containing anterior Y suture; (*6*) inner layer of posterior half of fetal nucleus, containing posterior Y suture; (*7*) posterior surface of fetal nucleus; (*8*) posterior surface of adult nucleus; (*9*) posterior line of disjunction; and (*10*) posterior capsule. (Reprinted with permission from CD Phelps. Examination and Functional Evaluation of the Crystalline Lens. In TD Duane, Clinical Ophthalmology [Vol 1]. Hagerstown, MD: Harper & Row, 1978.)

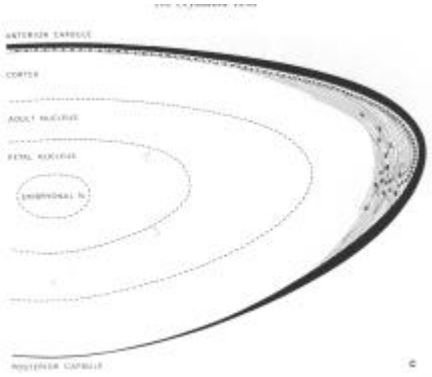

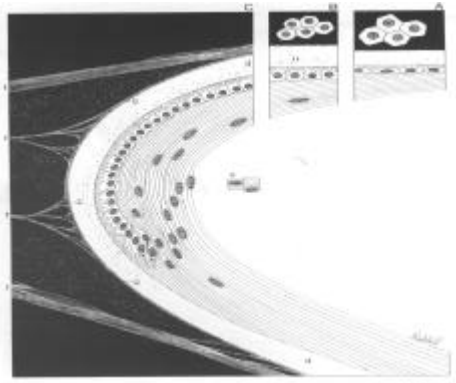

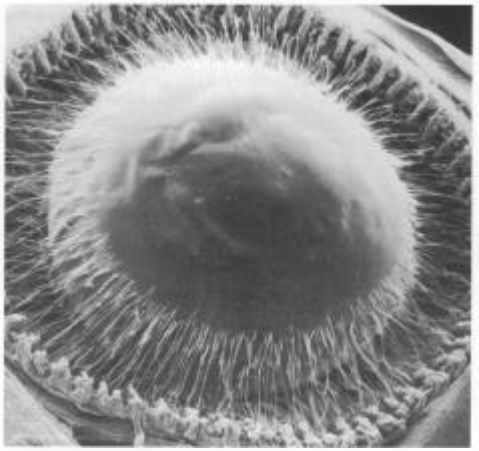

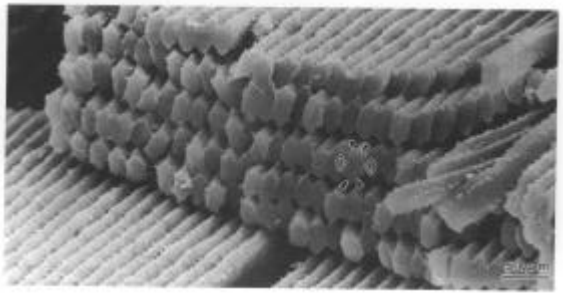

2.1.2.5 Lens (n=1.41 nucleus, n=1.38, cortex): It is the most remarkable of the optical components of the eye. It is built up from fine fibers. The lens is a gradient-index optical component. The index gradients, together with the aspherical form of its external and isoindicial surfaces may help to reduce aberration, particularly spherical aberration.

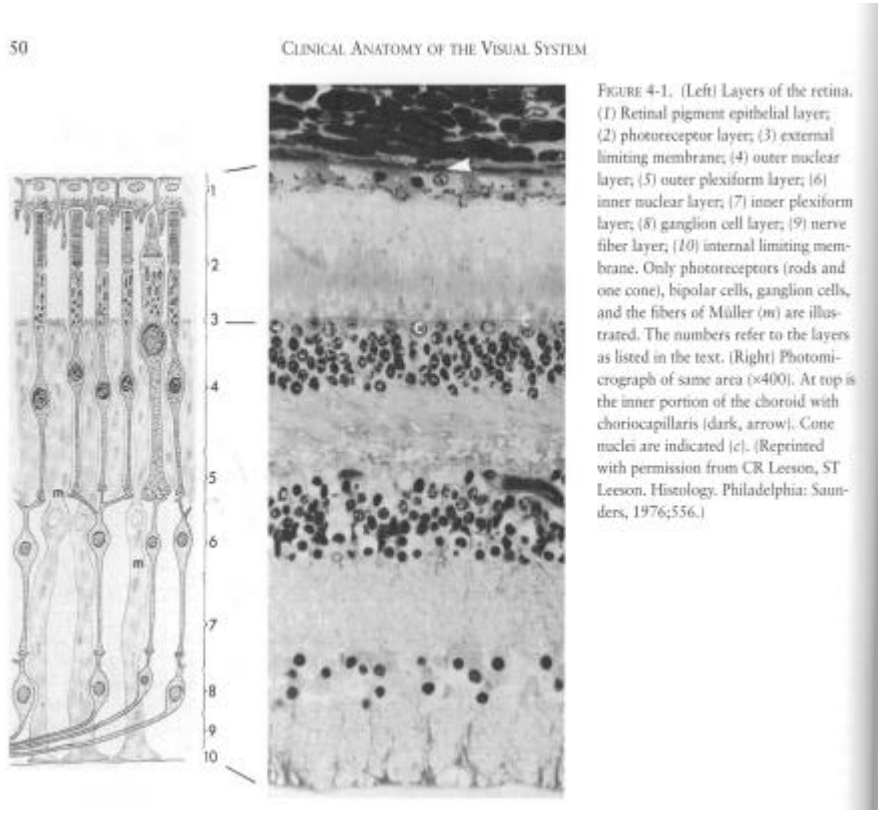

FIGURE 4-1. (Left) Layers of the retina. (1) Retinal pigment epithelial layer; (2) photoreceptor layer; (3) external limiting membrane; (4) outer nuclear layer; (5) outer plexiform layer; (6) inner nuclear layer; (7) inner plexiform layer; (8) ganglion cell layer; (9) nerve fiber layer; (10) internal limiting membrane. Only photoreceptors (rods and one cone), bipolar cells, ganglion cells, and the fibers of Müller (*m*) are illustrated. The numbers refer to the layers as listed in the text. (Right) Photomicrograph of same area (×400). At top is the inner portion of the choroid with choriocapillaris (dark, arrow). Cone nuclei are indicated (*c*). (Reprinted with permission from CR Leeson, ST Leeson. Histology. Philadelphia: Saunders, 1976;556.)

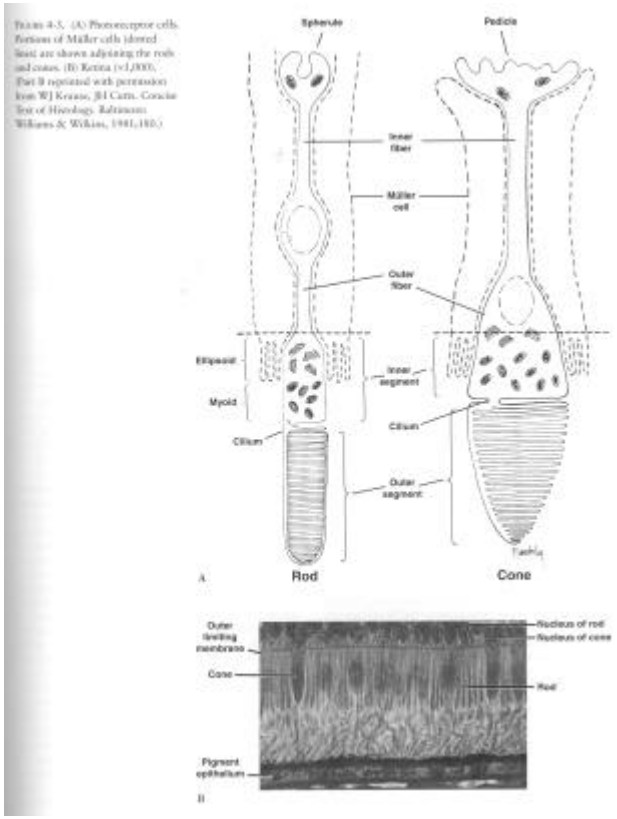

2.1.2.6 Retinal: It is actually an extension of the brain and consisting 6 layers of cells. There are two types of photoreceptor cells, rods (120M, Scotopic B/W night vision) and cones (6 M, Photopic color day vision) cells, which names for their shape. Forming image within certain focal length of eye.

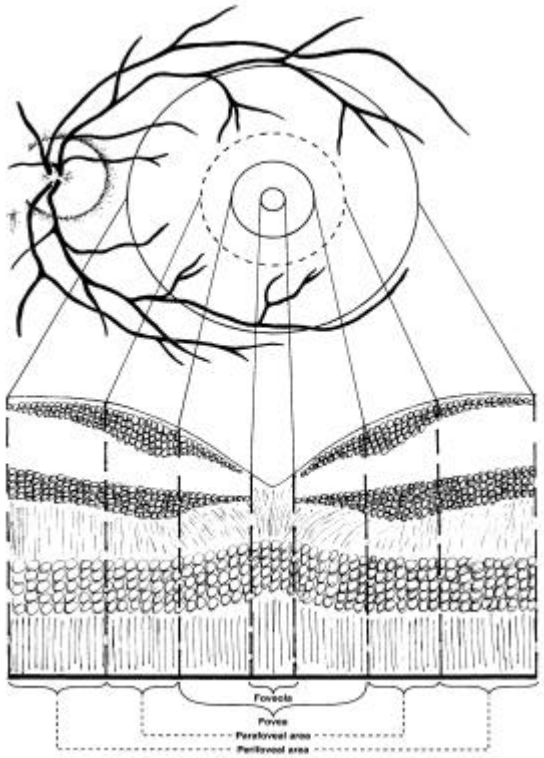

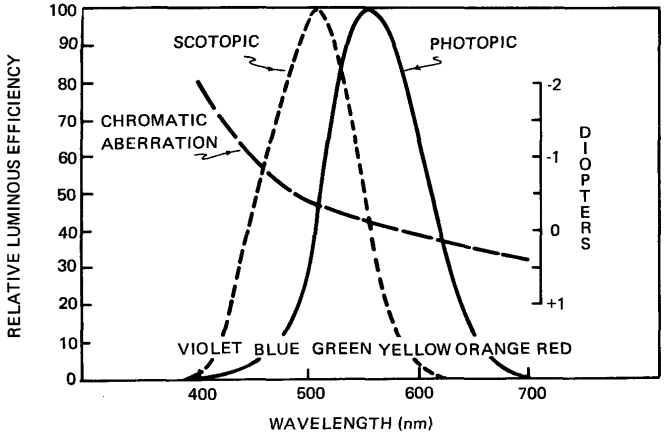

Figure 3-12. The scotopic (night) and photopic (day) responses of the eye. The CIE Function V_λ (photopic) and V'_λ (scotopic) for the CIE standard observer are illustrated as a function of wavelength. Peak rod sensitivy (scotopic) occurs at approximately 500 nm. Also shown is the variation of chromatic aberration as a function of wavelength. Notice the strong chromatic aberration existing in the short wavelength (blue) end of the spectrum. (Adapted from the Military Optical Design Handbook, 1962).

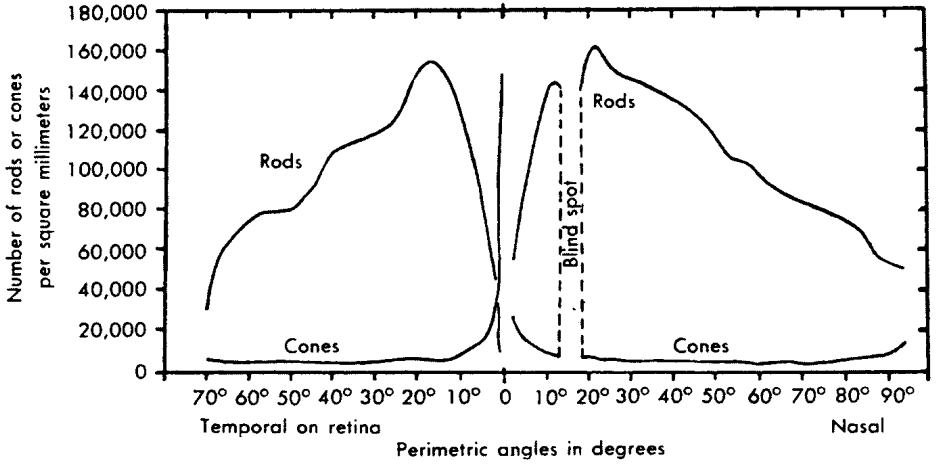

2.1.2.7 The Choroid: about 250 um thickness. It contains large (10-30 um) vessel for blood supply. It may act as a constant temperature warmer for the eye. There is a basement membrane between this layer and Bruch's membrane to keep the blood cells leak out to the interstitial tissue. The break off between these two layers is the major result in magnification of an originally slight trauma into serious retinal injury.

2.1.2.8 The Sclera: It is the dense, fibrous shell of the eye. To some extent, it functions to maintain the rigidity of the eyeball other than the internal pressure (10 mmHg).

2.1.2.9 Optical properties of the eye: The refractive power of the eye rests in the

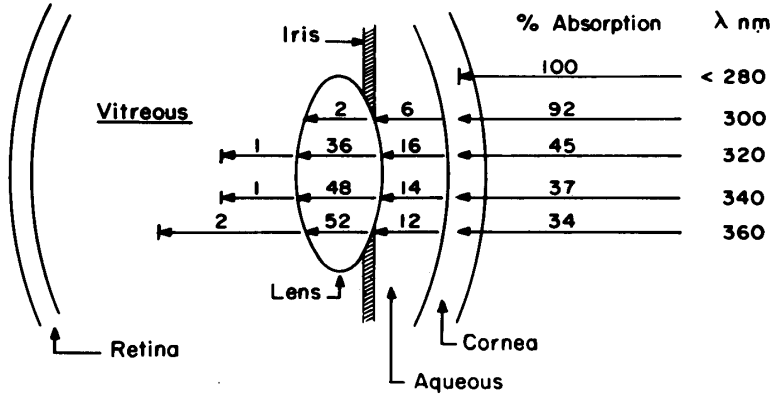

Figure 4-5. Schematic of absorption of ultraviolet radiation in the ocular media. Values represent the percent of ultraviolet radiation incident upon the corneal surface that are absorbed by various layers, redrawn from a figure by Matelsky, 1969. Based on data by Boettner and Wolter, 1962.

air-to cornea interface. (cornea 1.376) . The lens of the eyes actually provides only a 30% additional refractive power. The refractive power of the cornea and lens is often expressed in terms of diopters (D), which is the reciprocal of the effective focal length in meters. The total refractive power of the relaxed normal eye is around 59 D (f = 17 mm). The cornea alone provides a refractive power of about 45 D. (Q: The effect of under water without class) The amount of light, spectral distribution and polarization characteristics of the light reaching the retina are modified with respect to the original stimulus in a way that depends upon the transmittance characteristics of the eye. Light may be lost by spectrally varying

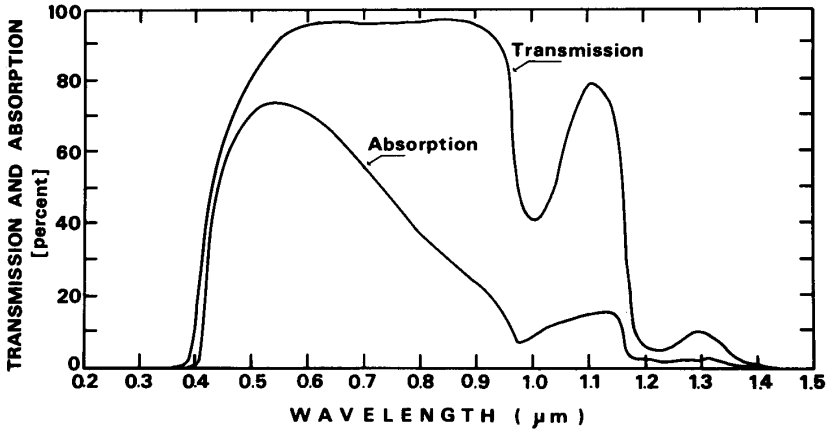

Figure 3-14. Optical spectral transmission of the human eye and absorption of light energy in the retina and choroid as a function of equal corneal spectral irradiance. The upper curve of spectral transmission would be used in calculating a retinal irradiance. The lower curve would be used to calculate retinal absorbed dose rate (from the data of Geeraets and Berry, 1968).

reflection, absorption, and scattering in any of the optical media anterior to the receptor out segment. Loss by Fresnel reflection at any boundary of different refractive indices n_1 and n_2 is $[(n_1- n_2)/(n_1+ n_2)]^2$. The loss ranges from 3~4 % up to 15 % at normal incidence and extreme angle. Wavelength-dependent absorption and scattering have much greater impact on the overall spectral transmittance, with the light losses occurring primarily in the cornea, lens and retina. It shows a rapid rise in transmittance at around 400 nm followed by high values through the visible and near infrared, the transmittance then falls again with a series of well-marked absorption bands to decline to zero at about 1400 nm. The light is further attenuated by the retina itself before it reaches the receptor outer segments. Not only is there some loss due to scattering and reflection, contributing some 30% of the total light scatter within the eye but there are further scattering effects from the retinal blood vessels region, the macular pigment, extending over the central few degrees of the retina and lying

anterior to the receptor outer segments absorbs heavily at short wavelengths. There are both spherical and chromatic aberration due to large pupil size. The average person can detect the separation between two point images separated by a visual angle of approximately one minute of arc (4.5 – 5 um), which is far better than the theoretical limit of airy disc (6.9 um, for a 3 mm pupil at 500 nm). d_r ? 2.44? ? ? f_e / d_e, d_e is the diameter of the eye's pupil, ? is the wavelength of the light, and f_e is the eye's effective focal length.

2.2 Effect of Optical Radiation on Biological Tissues and Safety

The effects of optical radiation on biological tissues constitute the requirements for Laser safety. Due to various optical properties of biological tissues, the hazards of laser operations vary greatly depending upon the exact type of laser (wavelength and duration) and its target applications. As the eye is the most sensitive and vulnerable to laser exposure, we will discuss the effects of laser on eye first and then list the safety requirements afterward.

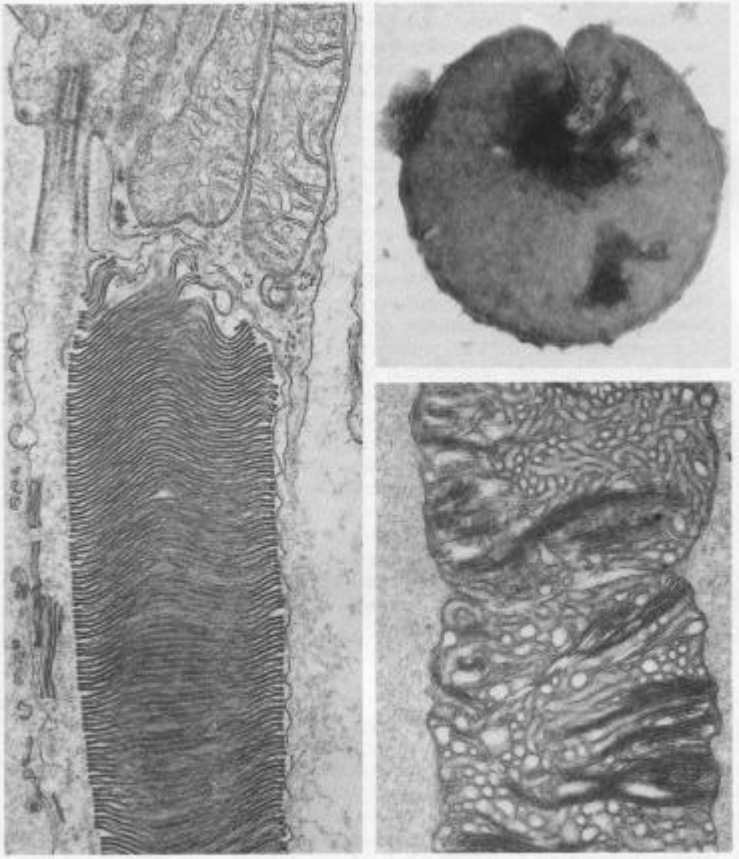

Figure 3-7. Ultrastructure of the rod outer segment in the retina. The left panel shows the junction of the discs with the inner segment. Upper right is a cross-section of a single disc and lower right is an expanded view of the discs following exposure to a high intensity laser which caused complete disorganization of the usual orderly stacked array. (Electron micrographs courtesy Dr. J. Marshall, Institute of Ophthalmology, London.)

The spectral distribution of optical radiation has differential effects on the eyes, thus we will list effects according to the spectral range.

2.2.1 UV effects:

2.2.1.1 Photochemical effects: As designations recommended by the CIE, there are three bands in this region of the optical radiation. UV-A (315-400 nm), which is a relatively less photobiologically active band; UV-B (280-315 nm), which is of most severe concern for skin exposure; UV-C (100-280 nm), which is particularly effective as

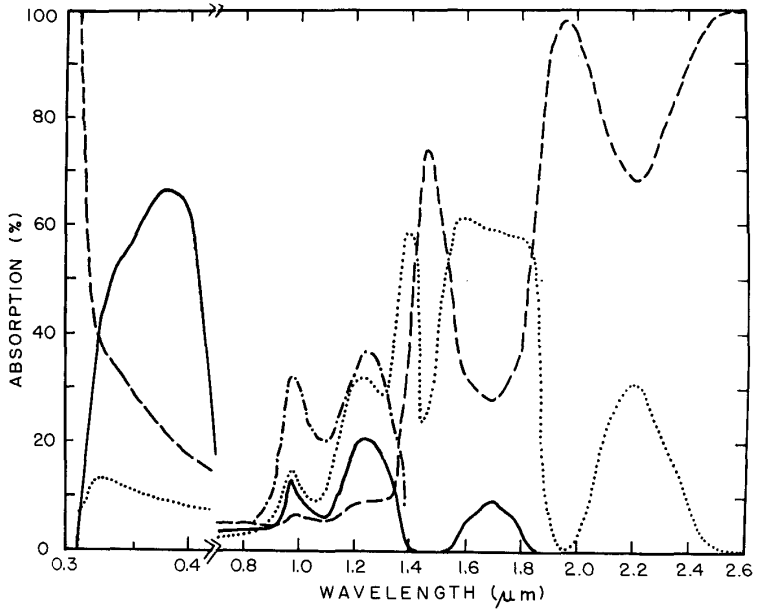

Figure 4-25. The spectral absorption of the Ocular Media for the Human Eye. Each portion of the ocular media, the cornea (- - - -), the aqueous humor (• • • •), the lens (———), and the vitreous humor (- • - •), absorb different portions of the incident optical radiation at different wavelengths. Very little is absorbed in the visible region, hence the break in the curves. Note the strong absorption of the lens in the near-ultraviolet region and the absorption of the vitreous in the 0.86-1.35 μm infrared region.

germicidal radiation.

2.2.1.2 Effects upon the cornea: UV-B and UV-C radiation are absorbed in the cornea and conjunctive and sufficiently high does will cause keratoconjunctivitis（角膜結膜炎）. From the action spectrum, the photochemical and biochemical mechanism of photokeratitis might be due to the active chromophores of albumins（白蛋白）and ? ?? globulins（球蛋白）, and the action spectrum of nucleoproteins DNA (265-275 nm).

2.2.1.3 Effects on the Lens: The lens has much the same sensitivity to UV as the cornea. However, the cornea is such an efficient filter for UV-C that little if any reaches the lens except at levels where the cornea is also injured. The radiation of UV and IR might contribute to the aging of the lens and the formation of cataract, which might be due to the activation of tryptophan (UV-A, >10-300 J/cm^2).

2.2.2 VIS-NIR (400-1400 nm): Its effects mainly on the retina through the energy absorption (photothermal effect). However, it is also dependent upon the exposure duration. The interaction modes will switch from photothermal to photomechanical as the pulse duration getting shorter (psec).

2.2.3 IR (IR-B 1.4 – 3 um, IR-C 3 um – 1 mm): The injury mechanism is largely thermal and absorbed by the ocular media. The adverse biological effects are infrared cataracts, flash burns, and heat stress. Above 2 um, the cornea can absorb significantly. Infrared laser (e.g. CO_2

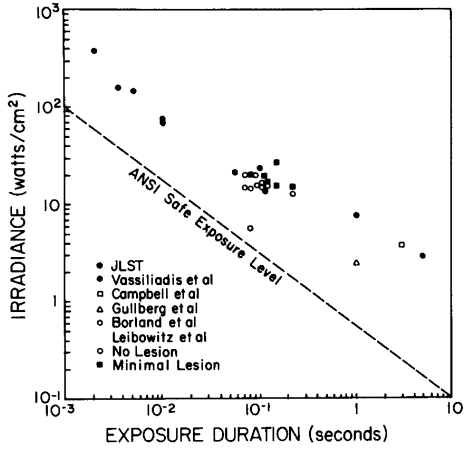

Figure 4-26. Thresholds for corneal injury from CO_2 laser radiation. The collected data of Stuck and colleagues of the US Army (JLST), much of it unpublished, is compared to the published threshold data of Vassiliadis (1971), Campbell *et al.* (1968), Goldberg *et al.* (1966), Borland *et al.* (1971), and Liebowitz and Peacock (1969). The range of data for the same exposure durations is thought to be due largely to the use of different corneal image sizes, and the two lowest points are believed the result of hot spots in a multimode laser irradiance pattern. Collation of data courtesy of Mr. Bruce Stuck, Letterman Army Institute of Researcch.

(10.6 um)) having CW output irradiances of the order of 10 W/cm^2 or greater could produce corneal lesions by delivering at least 0.5 to 10 J/cm^2.

2.3 Laser Safety Standards:

2.3.1 ACGIH:

2.3.2 ANSI Z-136:

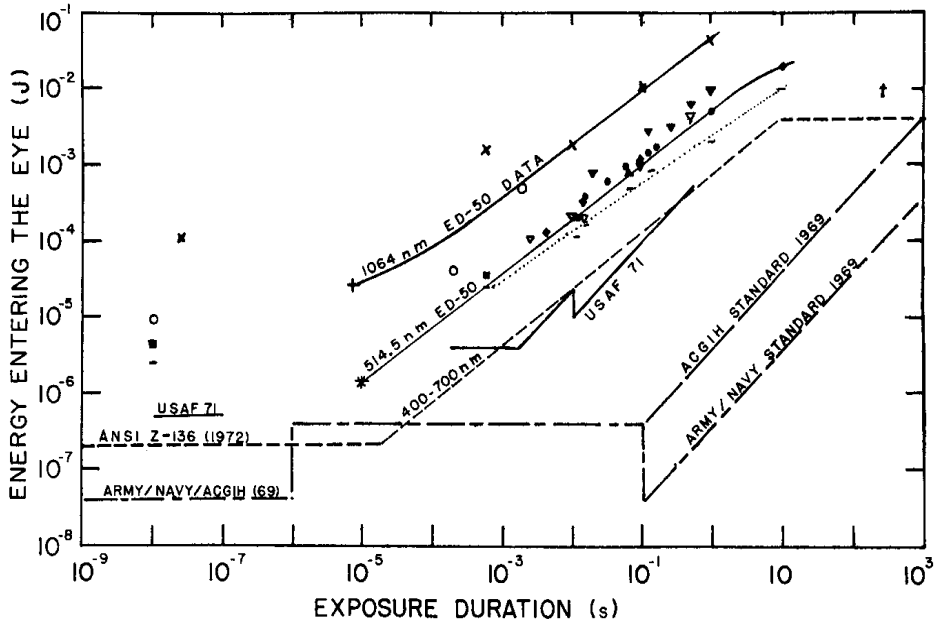

Figure 7-1. Intrabeam exposure limits for visible and infrared laser exposures. Evolution of intrabeam exposure limits for visible and IR-A laser radiation. The ED_{50} (50% probability of damage) values for ophthalmoscopically visible retinal lesions are shown for two wavelengths: 514.5 and 1064 nm. Data points are for minimal image sizes from: Ham *et al.* (1970) for 632.8 nm (▼); Dunsky and Lappin (1971) for 568 nm (●); Bresnick *et al.* (1970) for 514.5 nm (▲); Vassiliadis *et al.* (1971) for 532 nm (■) , and for 694.3 nm (○); Vassiliadis *et al.* for 514.5 nm (◇); Lappin (1970) for 632.8 nm (▽); Naidoff and Sliney (1973) for a welding arc point source (+); Skeen *et al.* (1972a) for 1064 nm (x); and Skeen *et al.* (1972b) for 514.5 nm (*). Points marked (-) indicate lowest reported injury values. Note how the later exposure limits fitted the trends of injury data more closely. From Wolbarsht and Sliney, 1974.

2.3.3 Classification:

2.3.3.1 Class IV: High Power Laser

2.3.3.2 Class III: Medium Power Laser (>5 mW)

2.3.3.3 Class II: Low-Power Laser (< 5 mW, 2.5 mW/cm^2 for a 0.25 s exposure)

2.3.3.4 Class I:

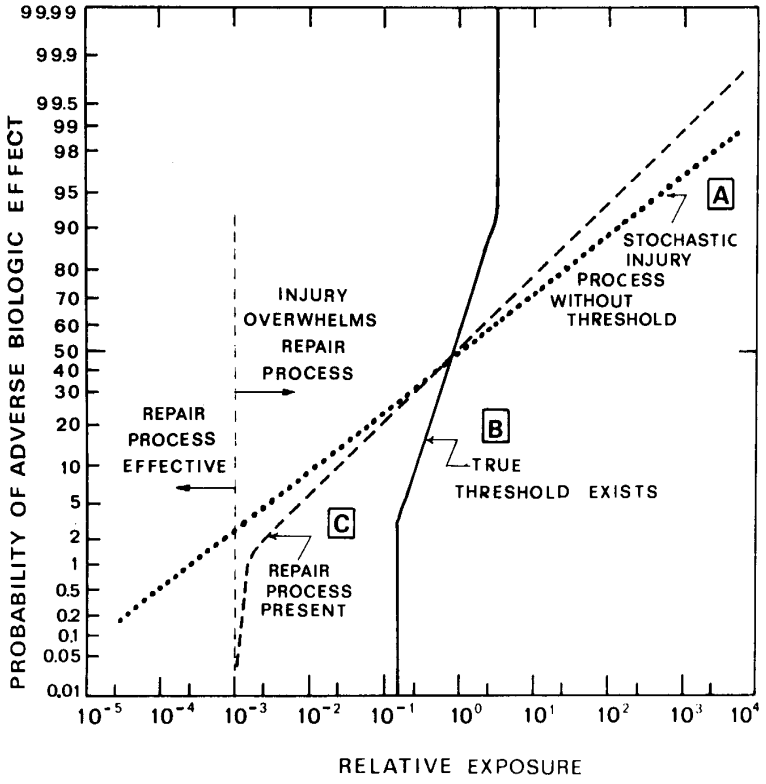

Figure 7-2. Biological thresholds and tissue repair processes. The concept of "threshold" for a biologic effect. Three types of idealized exposure dose response functions are shown. Line A represents an injury process without repair where cumulative exposure would increase the chance of injury and any single exposure would have a finite chance of causing injury. Curve C is similar to A except that a repair process creates a practical threshold; a real threshold does not exist due to errors in repair resulting in injury. Some scientists believe that carcinogenesis results from error-prone repair. Curve C is characteristic of damage produced by a pulse of thermal energy or by a photochemical reaction; a threshold exists and the spread of thresholds is due to biologic variability.

TABLE 8-1. Exposure Limits for Direct Ocular Exposures (Intrabeam Viewing) from a Laser Beam

Spectral Region	*Wave Length*	*Exposure Time, (t) Seconds*	*Exposure Limits*
UVC	200 nm to 280 nm	10^{-9} to 3×10^{4}	3 mJ/cm²
UVB	280 nm to 302 nm	"	3 "
	303 nm	"	4 "
	304 nm	"	6 "
	305 nm	"	10 "
	306 nm	"	16 "
	307 nm	"	25 "
	308 nm	"	40 "
	309 nm	"	63 "
	310 nm	"	100 "
	311 nm	"	160 "
	312 nm	"	250 "
	313 nm	"	400 "
	314 nm	"	630 "
	315 nm	"	1.0 J/cm²
	315 nm to 400 nm	10^{-4} to 10	$0.56\ t^{1/4}$ J/cm²
UVA	315 nm to 400 nm	10 to 10^{3}	1.0 J/cm²
	315 nm to 400 nm	10^{3} to 3×10^{4}	1.0 mW/cm²
Light	400 nm to 700 nm	10^{-9} to 1.8×10^{-5}	5×10^{-7} J/cm²
	400 nm to 700 nm	1.8×10^{-5} to 10	$1.8\ (t/\sqrt[4]{t})$ mJ/cm²
	400 nm to 549 nm	10 to 10^{4}	10 mJ/cm²
	550 nm to 700 nm	10 to T_1	$1.8\ (t/\sqrt[4]{t})$ mJ/cm²
	550 nm to 700 nm	T_1 to 10^{4}	$10\ C_B$ mJ/cm²
	400 nm to 700 nm	10^{4} to 3×10^{4}	C_B μW/cm²
IR-A	700 nm to 1049 nm	10^{-9} to 1.8×10^{-5}	$5\ C_A \times 10^{-7}$ J/cm²
	700 nm to 1049 nm	1.8×10^{-5} to 10^{3}	$1.8\ C_A\ (t/\sqrt[4]{t})$ mJ/cm²
	1050 nm to 1400 nm	10^{-9} to 10^{-4}	5×10^{-6} J/cm²
	1050 nm to 1400 nm	10^{-4} to 10^{3}	$9(t/\sqrt[4]{t})$ mJ/cm²
	700 nm to 1400 nm	10^{3} to 3×10^{4}	$320\ C_A$ μW/cm²
IR-B & C	1.4 μm to 10^{3} μm	10^{-9} to 10^{-7}	10^{-2} J/cm²
	1.4 μm to 10^{3} μm	10^{-7} to 10	$0.56\ \sqrt[4]{t}$ J/cm²
	1.4 μm to 10^{3} μm	10 to 3×10^{4}	0.1 W/cm²

not to exceed $0.56\ t^{1/4}$ J/cm²

C_A – See Fig. 8-8, Laser EL listing.

$C_B = 1$ for λ = 400 to 550 nm; $C_B = 10^{[0.015\ (\lambda - 550)]}$ for λ = 550 to 700 nm.

$T_1 = 10$ s for λ = 400 to 550 nm; $T_1 = 10 \times 10^{[\ 0.02\ (\lambda - 550)]}$ for λ = 550 to 700 nm.

For λ = 1.5 to 1.6 μm increase EL by 100.

TABLE 8-2. Exposure Limits for Viewing a Diffuse Reflection of a Laser Beam or an Extended Source Laser

Spectral Region	*Wave Length*	*Exposure Time, (t) Seconds*	*Exposure Limits*
UV	200 nm to 400 nm	10^{-3} to 3×10^{4}	Same as Table 8-3
Light	400 nm to 700 nm	10^{-9} to 10	$10\sqrt[3]{t}$ J/(cm²·sr)
	400 nm to 549 nm	10 to 10^{4}	21 J/(cm²·sr)
	550 nm to 700 nm	10 to T_1	$3.83\ (t/\sqrt[4]{t})$ J/(cm²·sr)
	550 nm to 700 nm	T_1 to 10^{4}	$21/C_B$ J/(cm²·sr)
	400 nm to 700 nm	10^{4} to 3×10^{4}	$2.1/C_B \times 10^{-3}$ W/(cm²·sr)
IR-A	700 nm to 1400 nm	10^{-9} to 10	$10\ C_A\sqrt[3]{t}$ J/(cm²·sr)
	700 nm to 1400 nm	10 to 10^{3}	$3.83\ C_A\ (t/\sqrt[4]{t})$ J/(cm²·sr)
	700 nm to 1400 nm	10^{3} to 3×10^{4}	$0.64\ C_A$ W/(cm²·sr)
IR-B & C	1.4 μm to 1 mm	10^{-9} to 3×10^{4}	Same as Table 8-3

C_A, C_B and T_1 are the same as in footnote to Table 8-1.

TABLE 8-3. Exposure Limits for Skin Exposure from a Laser Beam

Spectral Region	*Wave Length*	*Exposure Time, (t) Seconds*	*Exposure Limits*
UV	200 nm to 400 nm	10^{-3} to 3×10^{4}	Same as Table 8-1
Light &	400 nm to 1400 nm	10^{-9} to 10^{-7}	$2\ C_A \times 10^{-2}$ J/cm²
IR-A	400 nm to 1400 nm	10^{-7} to 10	$1.1\ C_A\sqrt[4]{t}$ J/cm²
IR-B & C	1.4 μm to 1 mm	10^{-9} to 3×10^{4}	Same as Table 8-1

$C_A = 1.0$ for λ = 400–700 nm; see Fig. 8-8 for greater wavelength values.